European Journal of Pharmaceutical Sciences 119 (2018) 22–30

Contents lists available at ScienceDirect

European Journal of Pharmaceutical Sciences

journal homepage: www.elsevier.com/locate/ejps

Population pharmacokinetics of oxaliplatin after intraperitoneal administration with hyperthermia in Wistar rats

M.I. Mas-Fuster[a,1], A. Ramon-Lopez[a,b,1], F.J. Lacueva[c], A. Arroyo[c], P. Más-Serrano[a,b,d], R. Nalda-Molina[a,b,*]

[a] Division of Pharmacy and Pharmaceutics, Department of Engineering, School of Pharmacy, Miguel Hernández University, San Juan de Alicante, Alicante, Spain
[b] Alicante Institute for Health and Biomedical Research (ISABIAL-FISABIO Foundation), Alicante, Spain
[c] Department of Pathology and Surgery, School of Medicine, Miguel Hernández University, San Juan de Alicante, Alicante, Spain
[d] Clinical Pharmacokinetics Unit, Pharmacy Department, Hospital General Universitario de Alicante, Alicante, Spain

ARTICLE INFO

Keywords:
Population pharmacokinetics
Oxaliplatin
Intraperitoneal chemotherapy
Peritoneal metastasis
Animal models

ABSTRACT

Background: The evaluation of the efficacy and toxicity of hyperthermic intraoperative peritoneal chemotherapy presents some difficulties, due in part to the lack of information about the pharmacokinetic behavior of the drugs administered in this procedure. The aim of this study was to characterize the population pharmacokinetics of hyperthermic intraoperative peritoneal oxaliplatin in Wistar rats and to evaluate the effect of treatment-related covariates dose, instillation time and temperature on the pharmacokinetic parameters.

Methods: Oxaliplatin peritoneal and plasma concentrations from 37 rats treated by either intravenous or intraperitoneal oxaliplatin administrations under different instillation times, temperatures and doses were analyzed according to a population pharmacokinetic approach using the software NONMEM V7.3®.

Results: Intraperitoneal (n = 115) and plasma (n = 263) concentrations were successfully described according to a two-compartment model with first order absorption. No significant effect of dose, temperature and instillation time on pharmacokinetic parameters was found. However, an abrupt decrease in the elimination process was observed, reflected in the structural pharmacokinetic model through a modification in clearance. The typical parameters values and the interindividual variability (CV %) in clearance, central and peripheral volume of distribution were 3.25 mL/min (39.1%), 53.6 mL (37.8%) and 54.1 mL (77.3%), respectively. Clearance decreased to 0.151 mL/min (39.1%) when the instillation was still ongoing, at 31.4 min. One of the possible reasons behind the clearance decrease would be an alteration of renal function due to surgery and/or hyperthermia.

Conclusions: This study described the deterioration of the drug elimination process due to the procedure, and estimated the time at which this deterioration is most likely to occur. In addition, dose, instillation time and temperature had no influence in the PK parameters.

1. Introduction

Peritoneal metastasis (PM) is a frequent site of dissemination of colorectal and gastric cancer and its treatment with systemic chemotherapy is considered palliative (Coccolini et al., 2013). However, a different treatment strategy including complete cytoreductive surgery (CRS) and hyperthermic intraoperative peritoneal chemotherapy (HIPEC), followed by systemic chemotherapy (Sugarbaker, 2005), has demonstrated to improve survival of selected patients with a limited peritoneal carcinomatosis index (Elias et al., 2014; Glehen et al., 2010; Verwaal et al., 2003).

The aim of CRS is to remove all visible tumor nodules within the abdominal cavity, while HIPEC eliminates the residual tumor cells. The addition of hyperthermia in the instillation solution has proved to increase the drug transport across membranes, accelerate the cell damage and generate free oxygen radicals (Hildebrandt et al., 2002). Oxaliplatin is one of the drugs that are used widely in HIPEC, with heat synergy and good depth penetration profile, around 1–2 mm (Elias et al., 2002; Rietbroek et al., 1997). However, oxaliplatin has a relatively low AUC ratio of 16, which is compensated by its rapid

* Corresponding author at: Division of Pharmacy and Pharmaceutics, Department of Engineering, School of Pharmacy, Miguel Hernández University, San Juan de Alicante, Alicante, Spain.
E-mail addresses: aramon@goumh.umh.es (A. Ramon-Lopez), fj.lacueva@umh.es (F.J. Lacueva), aarroyo@umh.es (A. Arroyo), jnalda@umh.es (R. Nalda-Molina).
[1] M.I. Mas-Fuster and A. Ramon-Lopez contributed equally to the article as first authors.

https://doi.org/10.1016/j.ejps.2018.04.004
Received 24 December 2017; Received in revised form 20 March 2018; Accepted 3 April 2018
Available online 04 April 2018
0928-0987/

absorption into the tumor nodule. That is why HIPEC procedure with oxaliplatin has a short duration of instillation.

The evaluation of the potential superiority of HIPEC over other treatments is troublesome due to the heterogeneity of the administration protocols among the different surgical teams worldwide, concerning the drug selection, dose, level of hyperthermia, carrier solution and duration of the instillation (Dubé et al., 2015; Ferron et al., 2008; Glockzin et al., 2014; Hompes et al., 2014; Muller et al., 2011; Ortega-Deballon et al., 2010; Pérez-Ruixo et al., 2014, 2013b; Robella et al., 2016; Sticca and Dach, 2003). However, few of them have evaluated the impact of those variables in the systemic absorption and the toxicity derived from this absorption (Pérez-Ruixo et al., 2014, 2013b; Ferron et al., 2008). Randomized clinical trials may adequately answer the questions related to the impact of components on different endpoints but, as pointed out by Sugarbaker, they are not likely to be completed in a timely manner, given the difficulties of being carried out (Elias et al., 2004; Sugarbaker and Van der Speeten, 2016). Instead, reviews establishing theoretical considerations for HIPEC as well as animal models are proposed as an alternative to the clinical studies (Gremonprez et al., 2014).

Development of suitable animal models contributes to evaluate the impact of the multiple components in HIPEC separately and gives useful information for future clinical research. To date, models in rat and pig have studied pharmacokinetics (PK), tumor growth and survival with different drugs (Gremonprez et al., 2014), given that PK models provide a better understanding of the involved mechanisms (Elishmereni et al., 2011). However, any of the studies with oxaliplatin considers the population PK approach in the data analysis.

Therefore, the aim of this study was to characterize the population PK model of hyperthermic intraoperative peritoneal oxaliplatin (HIPEO) in Wistar rats, by jointly analyzing the time course of oxaliplatin concentrations in peritoneum and plasma after intraperitoneal (ip) and intravenous (iv) administrations. The effect of treatment-related covariates dose, instillation time and temperature was also evaluated.

2. Material and methods

2.1. Animals

The PK of oxaliplatin was characterized in healthy male Wistar rats weighing on average 267 ± 22 g (mean ± standard deviation, SD), kept in the standard housing conditions with free access to water and a fasting day before surgery. The development of the experimental model, previously validated in rat (Pelz et al., 2005), was held at the Animal Experimentation Service of Miguel Hernández University of Elche (UMH). At the end of the procedure, rats were sacrificed. Care of the animals and drug administration was performed under veterinary control according to European Union Directive 2010/63/EU for animal experiments and with approval from the Ethics Committee of the UMH.

2.2. Study design

For the design of the experiment, the sample size was estimated to be 42 rats. Rats were randomly allocated in six groups (G1–G6) and submitted to different experimental conditions of temperature, instillation time or dose of oxaliplatin (Table 1). As a common procedure, all rats underwent laparotomy and intraperitoneal hyperthermic instillation (LIHI) with 100 mL of 5% dextrose solution under anesthetic conditions. Out of them, 36 were assigned to receive HIPEO administration, carried by the heated 5% dextrose solution, as used in HIPEC procedure.

In addition, to allow determination of the fraction of dose absorbed (F), six rats of one additional group (G7) were administered with one dose of iv oxaliplatin undergoing LIHI procedures, without adding oxaliplatin in the instillated intraperitoneal solution. This procedure ensured that iv administrations were done at similar surgical conditions to the HIPEC groups (Mas-Fuster et al., 2017).

The iv dose of oxaliplatin was 1.5 mg, based on previous experimental studies (Pestieau et al., 2001). Two different ip concentrations of 100 mg/L and 200 mg/L were evaluated. These concentrations are within the range of the concentrations used in clinical settings. No addition of carrier solution was done during the procedure in order to maintain original concentrations.

To evaluate the influence of temperature on oxaliplatin PK, three different instillation ranges of temperatures were selected: 38–40 °C, 40–42 °C and 42–43 °C. To evaluate the influence of instillation time on oxaliplatin PK, three different instillation times were selected: 30, 45 and 60 min.

Considering that the standard schedule applied in the clinical settings is the administration of oxaliplatin under 42 °C for 30 min (Elias et al., 2006), this schedule was selected as the standard conditions for G3, G4, G6 and G7.

2.3. Surgical procedure

All rats were operated under general anesthesia, induced by isoflurane (Isovet®) with oxygen vaporization. Intensity was regulated during the induction and maintenance phases (Fluovac®, Surgivet®). To avoid hypothermia induced by the anesthesia and by the laparotomy, rats were placed in the surgical area on a thermal blanket. Buprenorphine (Buprex® 0.3 mg/mL) was administered as analgesic at a subcutaneous dose of 0.05 mg/kg.

A permanent jugular vein catheterization was performed to all rats, as previously described (Liu et al., 2001), to allow blood sampling and also to administer iv oxaliplatin in G7. To balance the blood loss and to prevent the catheter obstruction, the catheter was rinsed with 0.2 mL of saline and filled with a 60% polyvinylpyrrolidone solution with heparinized saline (500 IU/mL) after each extraction.

In all the groups, a laparotomy from the pubic symphysis to the xiphoid cartilage was made to simulate the open Coliseum technique proposed by Sugarbaker, meaning open abdomen and closed circuit (Pelz et al., 2005; Sugarbaker et al., 1996). The skin of the abdomen was attached to a retractor structure and covered with saline solution coated dressings to avoid drying. Before the beginning of HIPEC, a choledochus ligature was done in all the rats in order to interrupt enterohepatic recirculation (Bastian et al., 2003; Huntjens et al., 2008; Roberts et al., 2002).

To perform recirculation of the solution, inlet and outlet drains were placed in the abdominal cavity, creating a closed circuit with the reservoir. The volume of the instillation solution was 100 mL of 5% dextrose. The instillation solution was heated by using a thermostatic bath (JpSelecta®). Once the reservoir volume reached the target temperature, recirculation of the solution started for the corresponding instillation times at 50 mL/min using an infusion pump (Masterflex® L/S EasyLoad 77202-50) (Fig. 1).

Temperature of the instillation solution in the abdominal cavity was monitored during the procedure. Once the HIPEC finalized, volume remaining in the peritoneal cavity was drained and the abdominal cavity was closed.

2.4. Collection of samples and bioanalytical procedure

Blood samples were taken after the administration of oxaliplatin at times 1, 10, 20, 30, 45, 60, 90, 150, 270 and 510 min and the total volume of these samples was kept to 0.2 mL with volume replacement during each sample extraction. Three peritoneal fluid samples per rat were taken, one at the beginning of the instillation, in order to know the actual initial peritoneal concentration of oxaliplatin, one in the middle of the procedure and one at the end of the HIPEC, depending on instillation time scheduled. Samples were collected in heparin tubes, immediately centrifuged for 10 min at room temperature and stored at

Table 1
Experimental groups according to doses, instillation time and temperatures. n: number of subjects.

Oxaliplatin route of administration	Temperature (°C)	Instillation time (minutes)	Dose (mg)		
			10	20	1.5
Intraperitoneal	38–40	30′	G1 (n = 6)		
	40–42	30′	G2 (n = 6)	G6 (n = 6)	
		45′	G3 (n = 6)		
		60′	G4 (n = 6)		
	42–43	30′	G5 (n = 6)		
Intravenous	40–42	30′			G7 (n = 6)

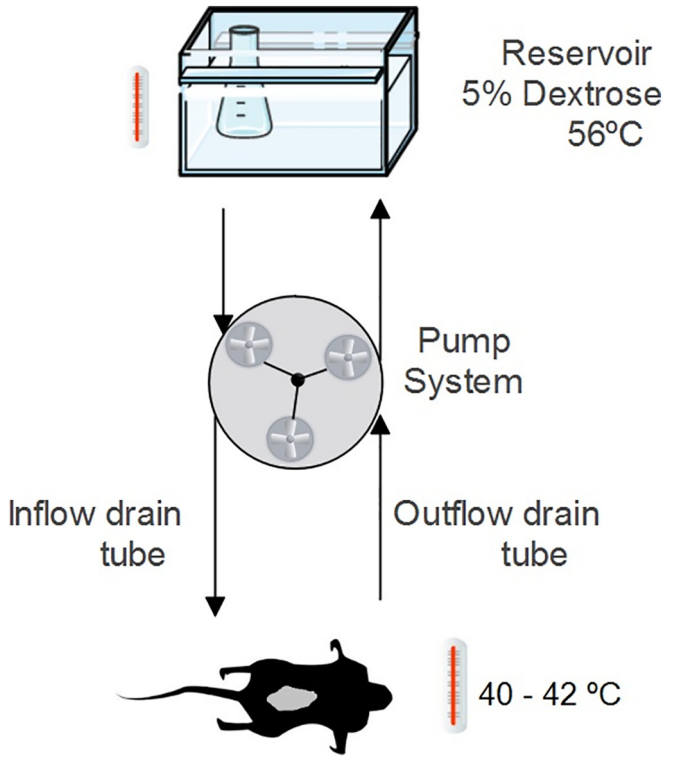

Fig. 1. Diagram of the experimental setup. One inflow and one outflow drain tubes were placed in the abdomen and connected to the pump system.

−20 °C until their analysis.

Total platinum was measured by a validated graphite furnace atomic absorption spectrophotometry method (Escudero-Ortiz et al., 2014). The analytical technique employed has a limit of quantification of 0.06 mg/L of oxaliplatin. All the results were expressed as oxaliplatin concentrations in mg/L.

2.5. Pharmacokinetic model development

2.5.1. Software

A population PK modeling approach was applied to the data using the first order conditional estimation (FOCE) method implemented in NONMEM version 7.3 (Beal et al., 2009), with the ADVAN 6 routine. Post-processing of the model results and diagnostic plots were performed with R 3.3.2 (R Core Team, 2016), implemented in R-studio (RStudio Team, 2015).

2.5.2. Structural model building

Based on a preliminary graphical analysis, HIPEO was assumed to be absorbed into the plasma according to a linear process, characterized by the first order absorption rate constant (k_a). k_a was calculated as a secondary parameter of the peritoneum to plasma clearance (Q_1) and the volume of distribution in the peritoneum, considered as V_1, fixed to 100 mL. F was included in the structural model, as a parameter of the differential equations.

An open, two-compartment model with linear elimination and linear distribution from the central to peripheral compartment (compartments 2 and 3, respectively) was selected to describe the oxaliplatin plasma concentrations after ip and iv administrations. This model was parameterized in terms of clearance (CL), central volume of distribution (V_2), intercompartmental clearance (Q_2) and volume of distribution of the peripheral compartment (V_3).

Preliminary graphical analysis showed a sharp inflection point, where the oxaliplatin plasma concentrations-time curve tends to increase before the end of instillation and thus, before the achievement of the maximum drug plasma concentration (C_{max}). Initial hypothesis for this phenomenon were based on the change in disposition processes at a certain time or the increase of the permeability of the peritoneum, causing the corresponding increase in the oxaliplatin plasma concentrations. These hypotheses were translated into a step function in time, consisting on a sigmoid function with high sigmoidicity factor (Hénin et al., 2012) (Eq. (1)). The step function was used to explore, in a continuous way, a quick change in distribution and/or elimination processes or the enhanced absorption process, reflected through a change in CL, V_2, V_3 or k_a:

$$STEP = \frac{TIME^{SIG}}{T_{50}{}^{SIG} + TIME^{SIG}} \quad (1)$$

where *TIME* is the dependent variable, T_{50} is the population estimate for the inflection time point, and *SIG* is the sigmoidicity factor, fixed to the value of 20. An example of the use of the step function is showed in Eqs. (2)–(4) for CL, modelled through the elimination rate constant (k_{el}).

$$CL_1 = THETA\,(1) * EXP(ETA(1)) \quad (2)$$

$$CL_2 = THETA\,(2) * EXP(ETA(1)) \quad (3)$$

$$k_{el} = \frac{CL1}{V_2} + \left(\frac{CL2}{V_2} - \frac{CL1}{V_2}\right) * STEP \quad (4)$$

2.5.3. Stochastic model building

Considering the population model, interindividual variability (IIV) of PK parameters between rats was assumed to follow a log-normal distribution in all population parameters, therefore, an exponential error model was used:

$$P_i = THETA * \exp(n_i) \quad (5)$$

Being *THETA* the population estimate for parameter *P*, P_i is the individual estimate and η_i is the normally distributed between-subject random variable with mean zero and variance ω^2.

Residual variability was evaluated using an additive error model after natural logarithmic transformation of the measured concentrations and model predictions, according to Eq. (6). Magnitude of the residual and interindividual variability was expressed as coefficient of variation (CV%):

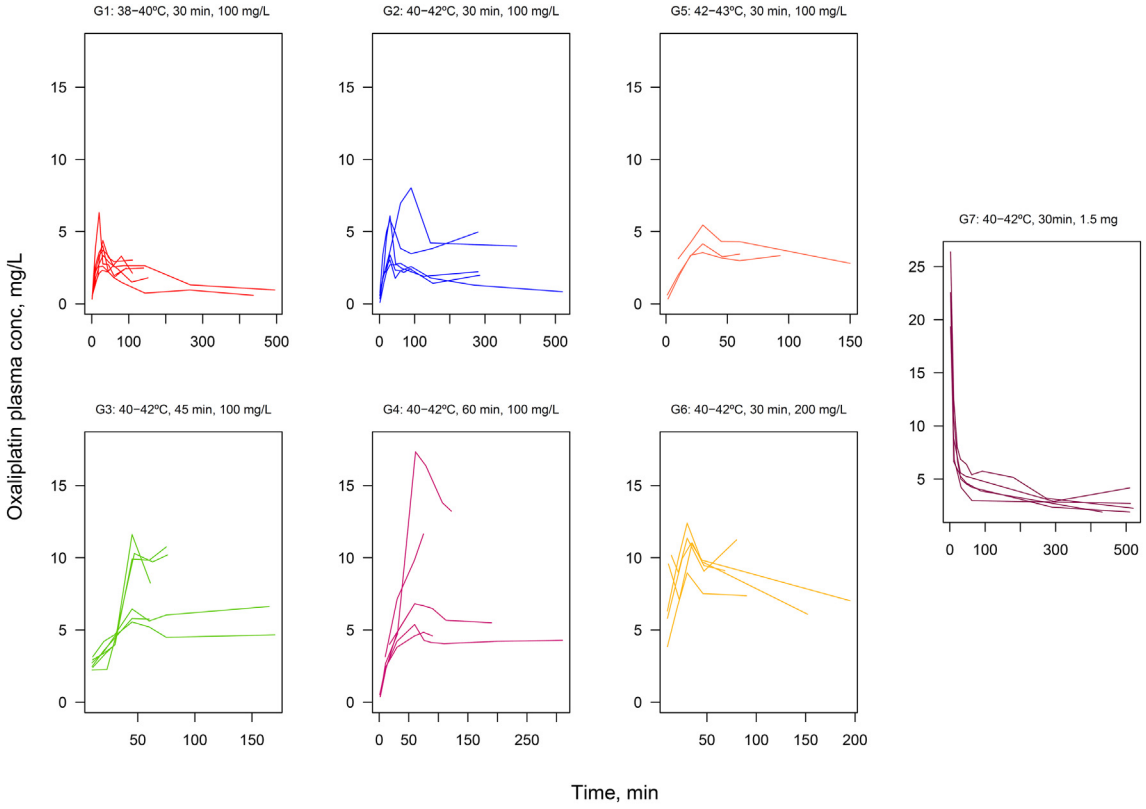

Fig. 2. Oxaliplatin concentration-time profiles for different scenarios of the study.

$$Y_{ij} = IPRED + W1{*}EPS(1){*}(1 - TYPE) + W2{*}EPS(2){*}TYPE \quad (6)$$

where Y is the jth observed concentration in the ith individual, $IPRED$ is the predicted concentration and $W1$ and $W2$ are the SD of the normally distributed residual random variable for peritoneal and plasma concentrations, respectively, with mean zero and variance, σ^2.

2.5.4. Model selection criteria

Model selection was based on the likelihood ratio test, using the improvement of the fit obtained for each model by NONMEM-generated minimum value of the objective function (MVOF); MVOF equal to minus twice the log likelihood of the data. The significance level was set to p-value = 0.01, one degree of freedom (df), which corresponds to a decrease in MVOF of ≥6.64 points after the inclusion of one parameter, assuming that the difference in minimum value of the MVOF between two nested models is χ^2 distributed.

In addition, improvement of the fit was assessed by the reduction in the IIV and residual variability, parameter relative standard errors (RSE %) < 50%, normalized prediction distribution errors (NPDE), correlation in parameter estimates and the examination of shrinkage. Based on the FOCE approximation, any individual observation with an absolute conditional weighted residual (CWRES) > 6 was identified as statistical outlier, as the CWRES has a mean zero and unit variance (Karlsson and Savic, 2007). The visual inspection of the classic goodness-of-fit plots was employed to detect bias in model fits: individual and population estimates vs observed concentrations as well as CWRES and NPDE vs time or population predicted values. Once the population PK model that best described the data was established, it was followed by covariate analysis and model validation.

2.5.5. Covariate analysis

In explaining part of the IIV, a covariate analysis was performed. In the absence of significant shrinkage, meaning lower than 30% (Savic and Karlsson, 2009), empirical Bayes estimates (EBE) of the inter-individual random effects were used to identify potential relationships between individual PK estimates and the experimental covariates, instillation time, temperature and dose. Dose was indirectly evaluated by the initial concentration in the peritoneal fluid. These covariates were first examined using scatterplots and then added to and removed from the population model in a stepwise manner (Wahlby et al., 2002). Again, a change of at least 6.64 points in the MVOF was required to consider the parameter significantly dependent of the covariate. Once the structural model was identified, EBE were computed.

To analyze the statistical power of the study design for detecting clinically relevant effects of these covariates on the PK parameters, 1000 stochastic simulations of the final model were performed, including an effect of 30% of change in the parameters for every 10 min of instillation time, 1 °C in the temperature or 10 mg/L in the dose. Then, the 1000 datasets simulated were fitted to the same model used in the simulation and also to the model without the covariate effect. Finally, the improvement in the MVOF was calculated to each simulation, and considered "positive" if > 6.64 or "negative" if not. The percentage of positives in the 1000 simulation for every covariate was considered to be the statistical power for each covariate.

2.5.6. Model qualification

A nonparametric bootstrap analysis (NPBS) (Efron and Tibshirani, 1993) and a prediction-corrected visual predictive check (pcVPC) (Bergstrand and Hooker, 2011) were used as internal evaluation methods to qualify the robustness and the predictive performance.

The NPBS was made after the generation of 1000 databases by random sampling with replacement by using the software WINGS for NONMEM (N. Holford, Version 616, Auckland, New Zealand). The mean and the 95% CI of the parameter estimates from the bootstrap replicates were compared with the estimated parameters from the original dataset. pcVPC was based on 1000 simulations of the oxaliplatin plasma concentrations from PK parameters obtained. Thus, observed and simulated oxaliplatin plasma concentrations were graphically compared.

Table 2
Mean plasma C_{max} (SD) and mean plasma $AUC_{0-\infty}$ (SD) for each group of rats.

Group	Dose (mg)	Temperature (°C)	Instillation time (min)	C_{max} (mg/L)	$AUC_{0-\infty}$ (mg∗min/L)
G1 (n = 6)	10	38–40	30	3.81 (1.33)	2210 (1050)
G2 (n = 6)	10	40–42	30	4.85 (2.13)	3500 (1540)
G3 (n = 6)	10	40–42	45	8.03 (2.91)	4370 (1370)
G4 (n = 6)	10	40–42	60	8.71 (4.88)	7830 (1090)
G5 (n = 3)	10	42–43	30	4.39 (0.98)	2620 (643)
G6 (n = 5)	20	40–42	30	11.0 (1.3)	6240 (480)
G7 (n = 5)	1.5	40–42	30	22.5 (2.5)	3730 (1360)

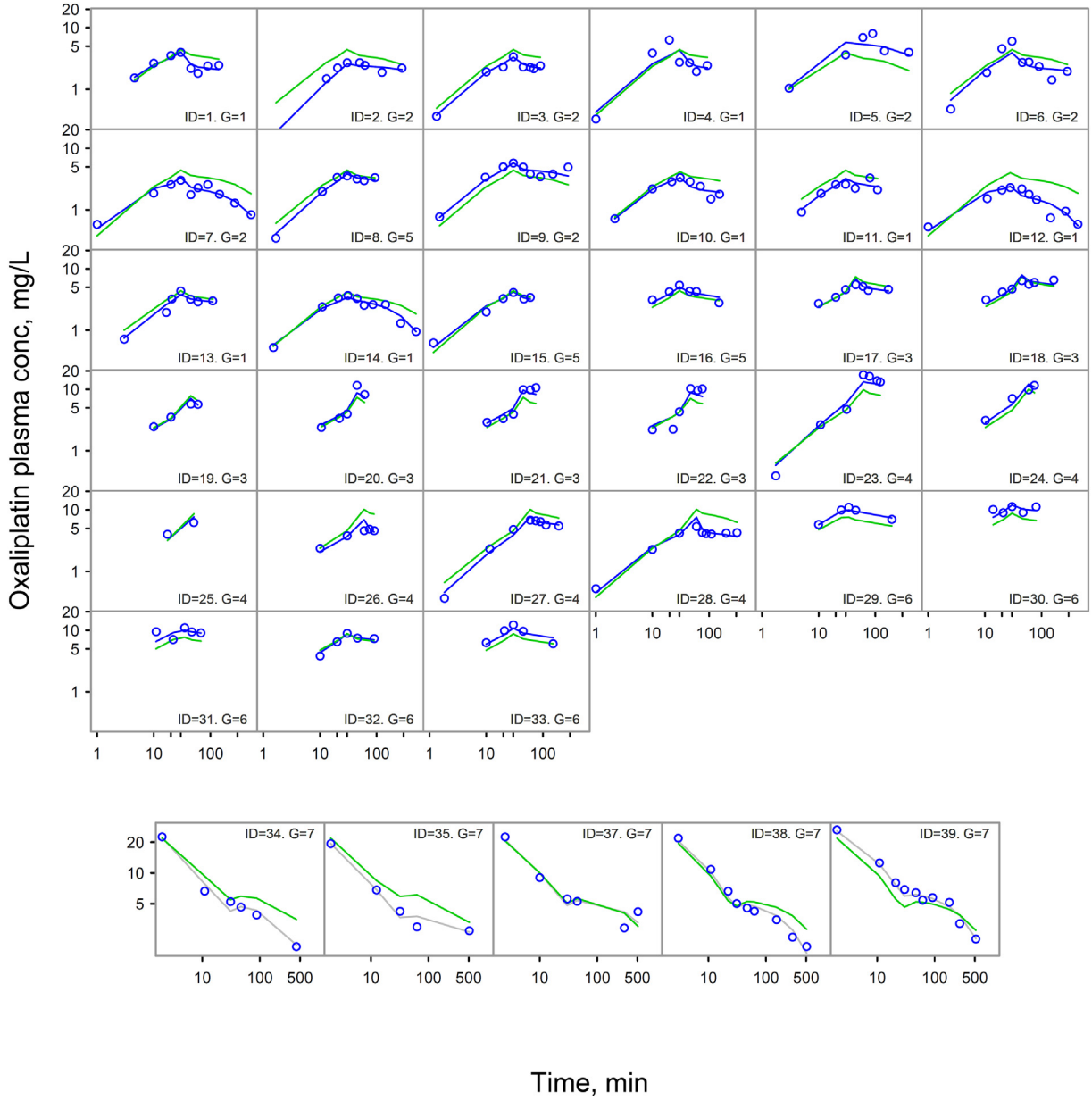

Fig. 3. Individual oxaliplatin plasma concentration-time profiles. Upper and lower panels represent the ip and iv oxaliplatin administrations, respectively. Circles represent the observed plasma concentrations while the blue and green lines represent the individual and the population predictions, respectively. (For interpretation of the references to colour in this figure legend, the reader is referred to the web version of this article.)

3. Results

3.1. Exploratory analysis

The experiment was well tolerated in all groups except G5. Rats of G5 showed a rapid deterioration after the procedure and died at early post-instillation times. Thus, for ethical reasons, and following the recommendations of the members of the ethical committee, experiments in these group were stopped, being the final sample size of G5 n = 3. One of the rats from G6 and one from G7 died during the surgical

Table 3
Parameter estimates and bootstrap analysis of the oxaliplatin population pharmacokinetic model.

Model parameters	Original dataset Estimate[a] (RSE)	Nonparametric bootstrap	
		Mean (RSE)[a]	95% CI
Fixed effect parameters			
CL_1 (mL/min)	3.25 (16.3)	3.18 (17.2)	2.00–4.14
CL_2 (mL/min)	0.151 (19.1)	0.154 (21.9)	0.0950–0.237
V_1 (mL)	100 FIX	100 FIX	–
Q_1 (mL/min)	0.864 (11.3)	0.866 (12.3)	0.660–1.09
V_2 (mL)	53.6 (13.4)	54.0 (14.3)	39.9–69.4
Q_2 (mL/min)	3.66 (28.4)	3.76 (34.0)	1.67–6.38
V_3 (mL)	54.1 (35.3)	54.5 (35.9)	22.1–98.8
T_{50} (min)	31.4 (2.70)	32.3 (8.80)	30.3–43.1
Between subject variability (η)[b]			
η_{CL}	39.1 (21.8)	36.9 (29.5)	15.2–59.3
η_{V2}	37.8 (24.5)	34.9 (29.7)	14.2–53.2
η_{V3}	77.3 (21.8)	78.9 (25.2)	46.9–125
Residual variability[b]			
Peritoneal	13.3 (9.64)	13.3 (9.64)	10.9–16.0
Plasma	20.0 (7.92)	19.7 (8.36)	16.7–23.0

Shrinkage values (%) of IIV in CL, V_2 and V_3 were estimated at 27.3, 18.1, and 17.6.

[a] Results expressed as parameter (RSE: relative standard error of the parameter estimate, %).

[b] Results expressed as coefficient of variation, CV %.

procedure for unknown etiology. Concentration-time profiles for all the scenarios are depicted in Fig. 2.

A total of 115 and 263 oxaliplatin concentrations from peritoneum and plasma, respectively, were available to describe oxaliplatin PK. Mean of the oxaliplatin C_{max} and mean area under the plasma concentration-time curve from zero to infinity ($AUC_{0-\infty}$) for each group are summarized in Table 2.

The peritoneal oxaliplatin concentrations observed during the instillation were in a range of 66.8–142 mg/L and 124–256 mg/L for 100 and 200 mg/L administrations, respectively. The evaporation of the carrier solution was not significant, since the residual volume after each procedure was measured and considered close to 100% of the initial volume in all the rats.

3.2. Population pharmacokinetic analysis

Oxaliplatin plasma concentrations after ip and iv administrations were jointly analyzed to allow an integrated modeling. The population PK analysis of oxaliplatin was best described by an open two-compartment disposition model with non-specific distribution to a peripheral compartment, linear elimination from the central compartment and first-order absorption from peritoneum to plasma, which agrees with other studies regarding HIPEO (Ferron et al., 2008; Pérez-Ruixo et al., 2013b).

However, the plasma concentration profile showed an inflection point between 30 and 45 min, while the instillation was still ongoing, increasing the slope (e.g. ID18, ID21, ID22 or ID28 in Fig. 3). A statistically significant decrease in the MVOF of −50.4 points ($df = 3$; p-value < 0.001) was observed when the final structural model included a decrease of the CL during the instillation, modelled through a step function on k_{el}. Including additional step functions in microconstants k_{23}, k_{32} or in k_a did not significantly improve the fit. This PK model successfully fitted the time course of oxaliplatin plasma concentrations after iv and ip administrations for different instillation times (Fig. 3).

In addition, other absorption models were tested, such as lag time or transit compartments models (Hénin et al., 2012; Savic et al., 2007). However, the fit of these models did not result in a significant decrease in the MVOF, and the change in the slope was not visually well captured. The change in the slope could have also been explained by the late absorption of part of the HIPEO dose, accumulated as a depot. This hypothesis was also tested by using models with a depot compartment. Although this model improved the MVOF and the goodness of fit plots, compared with a basic two-compartment structural model, it resulted over-parameterized, as well as the MVOF (ΔMVOF = 32.19 points, $df = 2$, p-value < 0.01) was worse than the final model proposed in this manuscript. Enterohepatic recirculation (Huntjens et al., 2008) was not tested as a structural part of the model because a choledochus ligature was performed in all the rats.

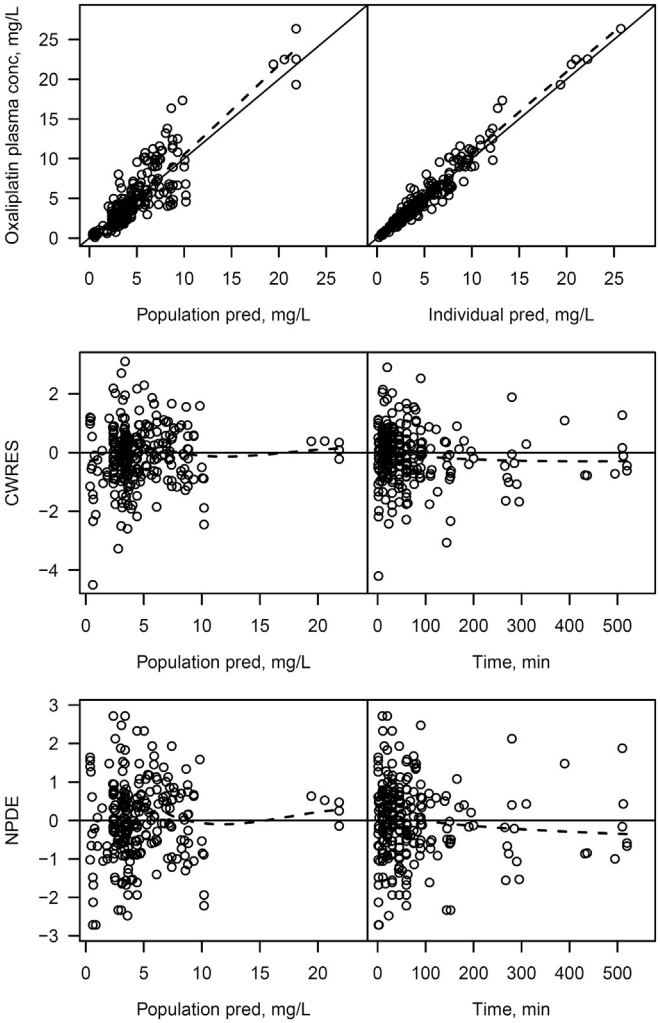

Fig. 4. Final model diagnostic plots of the PK model for oxaliplatin plasma concentrations. Upper panels, association between observed and predicted concentrations; middle and lower panels, CWRES and NPDE, respectively, vs time and population predicted values.

The final estimates of the PK model parameters and the results of the NPBS are presented in Table 3. IIV was estimated for CL, V_2 and V_3. The shrinkage values were lower than 30% in all the IIV. T_{50} is defined as the time at which the inflection point happened, and therefore the CL decreased. As the decreased in the CL has been modelled as a step function, two CL were estimated, e.g. CL_1 and CL_2, that run in the model when time is before or after T_{50}, respectively. T_{50} was estimated to be 31.4 min. This result agrees with the visual detection of this change in rats undergoing 45 or 60 min of instillation. Values of CL_1 and CL_2 were 3.25 mL/min and 0.15 mL/min, respectively. Volumes of distribution, V_2 and V_3, were estimated in 53.6 mL and 54.1 mL, respectively while k_a was estimated to be of 0.00864 min^{-1} (peritoneal $t_{1/2}$ = 80.2 min). Assuming dose-proportionality between 1.5 and 20 mg oxaliplatin doses, estimation of absolute bioavailability after ip

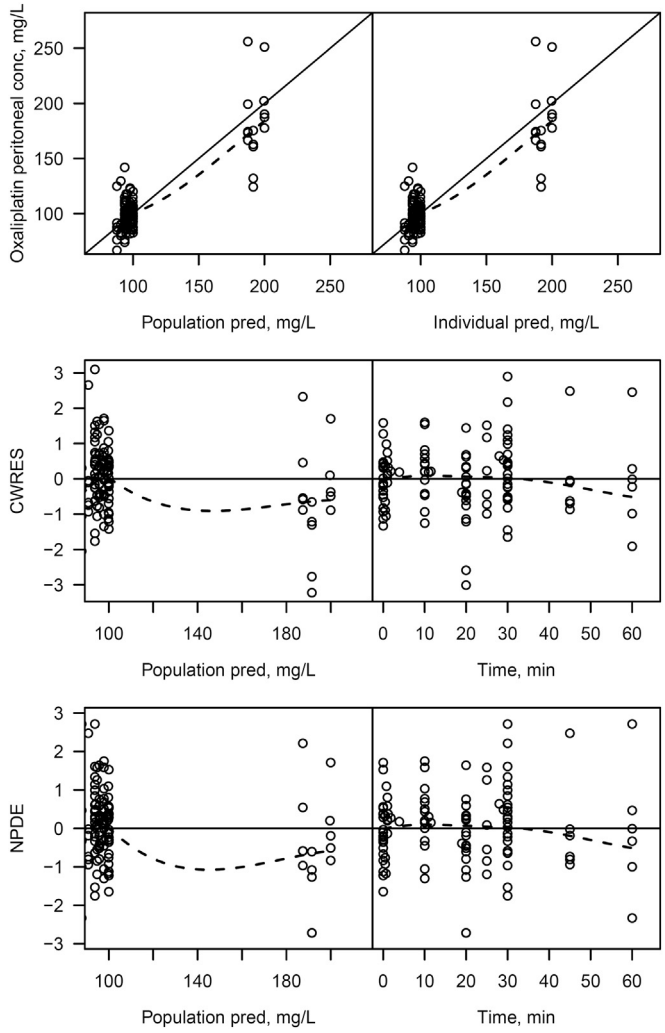

Fig. 5. Final model diagnostic plots of the PK model for oxaliplatin peritoneal concentrations. Upper panels, association between observed and predicted concentrations; middle and lower panels, CWRES and NPDE, respectively, vs time and population predicted values.

administrations was not significantly different from 100%.

3.2.1. Covariate analysis

Within the range of covariate values analyzed, the graphical and statistical analyses evidenced no effect of dose, temperature and instillation time on the PK model parameters. The statistical power calculated for the study design to detect clinically relevant changes in the PK parameters due to the studied covariates was > 80% in all the scenarios.

3.2.2. Model qualification

There was good association between the observed and predicted concentrations, indicating the absence of significant bias or model misfit. Similarly, no obvious trends in the CWRES or in the NPDE, indicating model inadequacy, were detected for the plasma concentrations (Fig. 4) or for the peritoneal concentrations (Fig. 5). In fact, the mean (± SD) and its confidence interval (CI) of the NPDE of peritoneal concentrations was 0.04 (95% CI −0.16:0.21) and 0.99 (95% CI 0.86:1.17), respectively. Likewise, for plasma concentrations these results were −0.0006 (95% CI −0.12:0.11) and 0.96 (95% CI 0.88:1.06), respectively. These results confirmed that observations were accurately predicted by the model without bias.

From 1000 replicates analyzed during the NPBS analysis, 2.2% failed to minimize successfully and were excluded from the analysis. The population estimates for the final model were similar to the mean of the NPBS replicates that minimized successfully and were contained within the 95% CI. The precision of the parameter estimates, based on the RSE% calculated from the bootstrap analysis, were lower than 36% for fixed effects and lower than 30% for random effects.

In addition, the results of the pcVPC depicted in Fig. 6 evidenced that the model developed was appropriate to describe the time course of oxaliplatin plasma concentrations and their associated variability.

4. Discussion

This is the first time that a population PK model for oxaliplatin after ip hyperthermic instillation has been studied in experimental models. The population PK of oxaliplatin was well described by a two-compartment model with non-specific distribution to a peripheral compartment, linear elimination from the central compartment and first-order absorption from peritoneum to plasma. Dose, instillation time and temperature had neither significant impact on PK parameters, according to the MVOF, nor impact in decreasing the IIV of the parameters. These results are in agreement with other studies (Bendavid et al., 2005; Ferron et al., 2008; Jacquet et al., 1998; Pestieau et al., 1998; Sørensen et al., 2014; Zakris et al., 1987). However, Piché et al. (2011) observed a decrease in systemic absorption as temperature increased, using a closed technique in HIPEC. The rise in the temperature in a closed technique may entail an increase of the vapor pressure in the peritoneal cavity, being difficult to assess whether decrease in systemic absorption is caused by the temperature or by the pressure level in the peritoneal cavity.

The increments in dose or instillation time produced a proportional increment in C_{max} and AUC in plasma, warranting dose-proportional pharmacokinetics. The AUC in plasma showed an increase in G2 compared to G1 that could indicate a temperature-dependency of oxaliplatin bioavailability. However, this hypothesis was not consistent with the AUC in G5 that was lower than G2.

The profile of HIPEO plasma concentrations was unusual in the rats from G3 and G4, these groups following instillation times higher than 30 min, with an increase in the slope while the instillation was still ongoing. In addition, these two groups registered the higher variability in the study. Thus, the structural model was updated to describe, for the first time, a deterioration of drug elimination mechanisms, reflected through a change in the parameter CL. These findings agree with the alteration of renal function attributed to surgery and/or hyperthermia observed in other studies (Ceresoli et al., 2016; Mustafa et al., 2007; Sladen, 1987). A previous study showed that rats undergoing a similar surgical procedure had significant lower CL and V_2 than those that were not submitted to surgery (Mas-Fuster et al., 2017). Moreover, there is no literature regarding the identification of the time at which this deterioration begins, neither at preclinical experiments nor in clinical settings, except for one study that evaluated the impact of the duration of the whole surgical procedure (van Ruth et al., 2004) including cytoreduction steps on the PK parameters. The CL_1 and CL_2 values obtained in our study are different from the value obtained in a previous experimental study in rats receiving oxaliplatin in similar surgical conditions (Mas-Fuster et al., 2017). However, it must be pointed out that the mean CL in our study was estimated to be 0.49 mL/min when no step function was added to the model, which agrees with the results obtained in that study.

Most of the surgical teams establish the instillation times of the drugs employed in HIPEC from an empirical basis. Some studies justified somehow the duration of the instillation, attending to its peritoneal $t_{1/2}$ (Ferron et al., 2008; Sugarbaker and Van der Speeten, 2016). But any study has considered the impact of the surgical procedure and the instillation on the PK parameters, and therefore, on the exposure of the drug and its toxicity. The knowledge of the time when the impact on the renal function becomes clinically relevant could be helpful and should

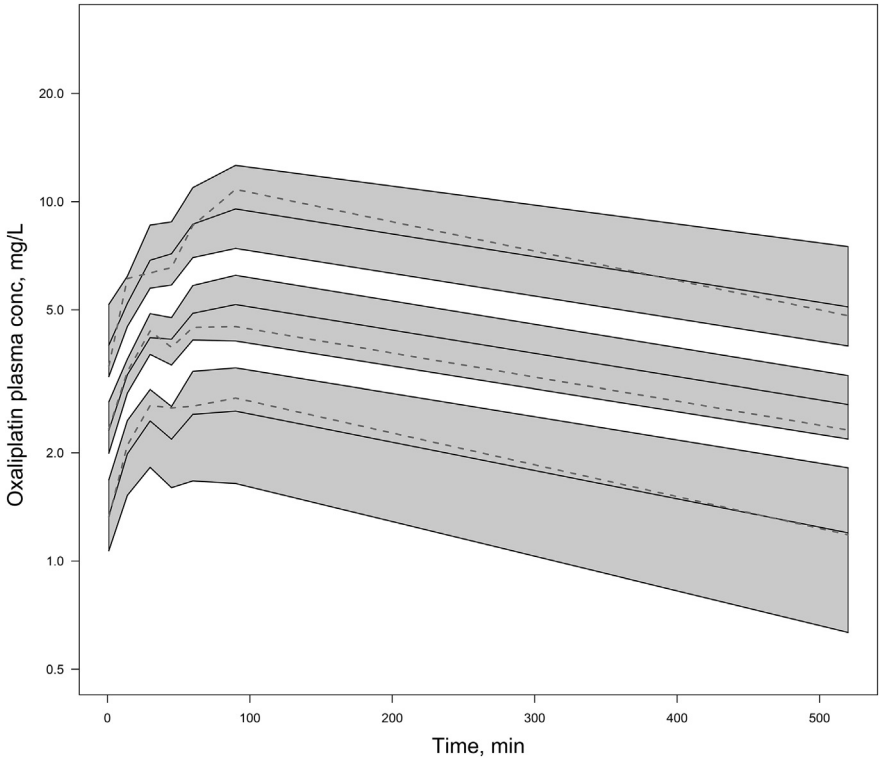

Fig. 6. Model validation. pcVPC, showing the 5th, 50th, and 95th percentiles of the observed values (dashed lines), and the 95% CI for the corresponding model-based predicted percentiles (solid lines).

be considered when choosing the duration of the instillation. However, clinical studies must be done to evaluate if this phenomenon also occurs in humans.

The use of total platinum instead of unbound platinum in PK analysis is supported by a previous study, where the correlation between total and unbound platinum plasma levels was high ($r^2 = 0.98$) (Brouwers et al., 2008). Moreover, another study also confirmed that the binding process for oxaliplatin in plasma is in the linear range of the Michaelis–Menten curve (Chalret du Rieu et al., 2014). In light of these results, the conclusions derived from our work should not be influenced by the moiety used in the analysis. Other PK studies in HIPEC have also used total platinum, instead of unbound platinum (Ferron et al., 2008; Pérez-Ruixo et al., 2016, 2013a, 2013b; Valenzuela et al., 2011).

One of the limitations of our study is related to the high mortality observed in G5, that can be attributed to the high level of hyperthermia applied to this group (Yonemura et al., 1996; Zakris et al., 1987). Thus, the results of the covariate analysis regarding temperature obtained in this study should be restricted to the range of 38 °C to 42 °C. In addition, this study has been conducted in healthy rats, with no peritonectomy performed, and therefore, actual conditions of cytoreduction were not completely recreated. The impact of the peritonectomy vs non-peritonectomy performance on PK parameters has not been studied previously, even though no changes in the PK have been reported related to the extent of peritonectomy in humans (de Lima Vazquez et al., 2003).

5. Conclusions

In conclusion, this study shows the deterioration of the drug elimination process due to the HIPEC procedure, and estimates the time at which this deterioration is most likely to occur. On the other hand, our results confirm that covariates dose, instillation time and temperature had no influence in the PK parameters, in the studied range. This model may help in the understanding of how HIPEC procedure affects PK parameters and may contribute in the construction of solid hypothesis for future clinical trials.

Ethics approval

Development of experimental model was held at the Animal Experimentation Service of Miguel Hernández University of Elche (UMH). Care of the animals and drug administration were performed under veterinary control according to European Union Directive 2010/63/EU for animal experiments and with approval from the Ethics Committee of the UMH.

Conflict of interests

The authors report no declarations of interest.

Acknowledgements

The authors would like to acknowledge the Animal Experimentation Service of San Juan de Alicante, UMH, for all the assistance received.

Funding

This study was funded by the Fundación Navarro Tripodi and from Proyecto Bancaja-UMH. The funding sources had no involvement in study design, collection, analysis and interpretation of data, in the writing of the report or in the decision to submit the article for publication.

References

Bastian, G., Barrail, A., Urien, S., 2003. Population pharmacokinetics of oxaliplatin in patients with metastatic cancer. Anti-Cancer Drugs 14 (10), 817–824.
Beal, S., Sheiner, L.B., Boeckmann, A., Bauer, R.J., 2009. NONMEM User's Guides. (1989–2009), Icon Development Solutions, Ellicott City, MD, USA.
Bendavid, Y., Leblond, F.A., Dubé, P., 2005. A study of the effect of temperature on the pharmacokinetic profile of raltitrexed administered by intraperitoneal route in the

rat. Med. Sci. Monit. 11 (1), BR1–5.
Bergstrand, M., Hooker, A.C., 2011. Prediction-corrected visual predictive checks for diagnosing nonlinear mixed-effects models. AAPS J. 13, 143–151.
Brouwers, E.E., Huitema, A.D., Beijnen, J.H., et al., 2008. Long-term platinum retention after treatment with cisplatin and oxaliplatin. BMC Clin. Pharmacol. 17 (8), 7.
Ceresoli, M., Coccolini, F., Ansaloni, L., 2016. HIPEC and nephrotoxicity: a cisplatin induced effect? Eur. J. Surg. Oncol. 42 (6), 909–910.
Chalret du Rieu, Q., White-Koning, M., Picaud, L., Lochon, I., Marsili, S., Gladieff, L., et al., 2014. Population pharmacokinetics of peritoneal, plasma ultrafiltrated and protein-bound oxaliplatin concentrations in patients with disseminated peritoneal cancer after intraperitoneal hyperthermic chemoperfusion of oxaliplatin following cytoreductive surgery: correlation between oxaliplatin exposure and thrombocytopenia. Cancer Chemother. Pharmacol. 74 (3), 571–582.
Coccolini, F., Gheza, F., Lotti, M., Virzi, S., Iusco, D., Ghermandi, C., et al., 2013. Peritoneal carcinomatosis. World J. Gastroenterol. 19 (41), 6979–6994.
Dubé, P., Sideris, L., Law, C., Mack, L., Haase, E., Giacomantonio, C., et al., 2015. Guidelines on the use of cytoreductive surgery and hyperthermic intraperitoneal chemotherapy in patients with peritoneal surface malignancy arising from colorectal or appendiceal neoplasms. Curr. Oncol. 22 (2), e100.
Efron, B., Tibshirani, R., 1993. An Introduction to the Bootstrap. Chapman & Hall/CRC, New York.
Elias, D., Bonnay, M., Puizillou, J.M., Antoun, S., Demirdjian, S., El, O.A., et al., 2002. Heated intra-operative intraperitoneal oxaliplatin after complete resection of peritoneal carcinomatosis: pharmacokinetics and tissue distribution. Ann. Oncol. 13, 267–272.
Elias, D., Delperro, J.-R., Sideris, L., Benhamou, E., Pocard, M., Baton, O., et al., 2004. Treatment of peritoneal carcinomatosis from colorectal cancer: impact of complete cytoreductive surgery and difficulties in conducting randomized trials. Ann. Surg. Oncol. 11 (5), 518–521.
Elias, D., Raynard, B., Bonnay, M., Pocard, M., 2006. Heated intra-operative intraperitoneal oxaliplatin alone and in combination with intraperitoneal irinotecan: pharmacologic studies. Eur. J. Surg. Oncol. 32 (6), 607–613.
Elias, D., Goere, D., Dumont, F., Honore, C., Dartigues, P., Stoclin, A., et al., 2014. Role of hyperthermic intraoperative peritoneal chemotherapy in the management of peritoneal metastases. Eur. J. Cancer 50, 332–340.
Elishmereni, M., Kheifetz, Y., Søndergaard, H., Overgaard, R.V., Agur, Z., 2011. An integrated disease/pharmacokinetic/pharmacodynamic model suggests improved Interleukin-21 regimens validated prospectively for mouse solid cancers. PLoS Comput. Biol. 7 (9), e1002206.
Escudero-Ortiz, V., Duart-Duart, M.J., Pérez-Ruixo, C., Pérez-Ruixo, J.J., Valenzuela, B., 2014. Stability study of oxaliplatin and doxorubicin for intraperitoneal administration with hyperthermia. Farm. Hosp. 38, 154–161.
Ferron, G., Dattez, S., Gladieff, L., Delord, J.-P., Pierre, S., Lafont, T., et al., 2008. Pharmacokinetics of heated intraperitoneal oxaliplatin. Cancer Chemother. Pharmacol. 62 (4), 679–683.
Glehen, O., Gilly, F., Arvieux, C., Cotte, E., Boutitie, F., et al., 2010. Peritoneal carcinomatosis from gastric cancer: a multi-institutional study of 159 patients treated by cytoreductive surgery combined with perioperative intraperitoneal chemotherapy. Ann. Surg. Oncol. 17, 2370–2377.
Glockzin, G., Gerken, M., Lang, S.A., Klinkhammer-Schalke, M., Piso, P., Schlitt, H.J., 2014. Oxaliplatin-based versus irinotecan-based hyperthermic intraperitoneal chemotherapy (HIPEC) in patients with peritoneal metastasis from appendiceal and colorectal cancer: a retrospective analysis. BMC Cancer 14, 807.
Gremonprez, F., Willaert, W., Ceelen, W., 2014. Intraperitoneal chemotherapy (IPC) for peritoneal carcinomatosis: review of animal models. J. Surg. Oncol. 109 (2), 110–116.
Hénin, E., Bergstrand, M., Standing, J.F., Karlsson, M.O., 2012. A mechanism-based approach for absorption modeling: the gastro-intestinal transit time (GITT) model. AAPS J. 14 (2), 155–163.
Hildebrandt, B., Wust, P., Ahlers, O., Dieing, A., Sreenivasa, G., Kerner, T., et al., 2002. The cellular and molecular basis of hyperthermia. Crit. Rev. Oncol. Hematol. 43 (1), 33–56.
Hompes, D., D'Hoore, A., Wolthuis, A., Fieuws, S., Mirck, B., Bruin, S., et al., 2014. The use of oxaliplatin or mitomycin C in HIPEC treatment for peritoneal carcinomatosis from colorectal cancer: a comparative study. J. Surg. Oncol. 109 (6), 527–532.
Huntjens, D.R.H., Strougo, A., Chain, A., Metcalf, A., Summerfield, S., Spalding, D.J.M., et al., 2008. Population pharmacokinetic modelling of the enterohepatic recirculation of diclofenac and rofecoxib in rats. Br. J. Pharmacol. 153 (5), 1072–1084.
Jacquet, P., Averbach, A., Stuart, O.A., Chang, D., Sugarbaker, P.H., 1998. Hyperthermic intraperitoneal doxorubicin: pharmacokinetics, metabolism, and tissue distribution in a rat model. Cancer Chemother. Pharmacol. 41 (2), 147–154.
Karlsson, M.O., Savic, R.M., 2007. Diagnosing model diagnostics. Clin. Pharmacol. Ther. 82 (1), 17–20.
de Lima Vazquez, V., Stuart, O.A., Mohamed, F., Sugarbaker, P.H., 2003. Extent of parietal peritonectomy does not change intraperitoneal chemotherapy pharmacokinetics. Cancer Chemother. Pharmacol. 52 (2), 108–112.
Liu, J., Kraut, E.H., Balcerzak, S., Grever, M., D'Ambrosio, S., Chan, K.K., 2001. Dosing sequence-dependent pharmacokinetic interaction of oxaliplatin with paclitaxel in the rat. Cancer Chemother. Pharmacol. 50, 445–453.
Mas-Fuster, M.I., Ramon-Lopez, A., Lacueva, J., Compañ, A., Más-Serrano, P., Nalda-Molina, R., 2017. Impact of Laparotomy and Intraperitoneal Hyperthermic Instillation (LIHI) on the oxaliplatin pharmacokinetics after intravenous administration in Wistar rats. Cancer Chemother. Pharmacol. 1–7.
Muller, M., Chérel, M., Dupré, P.F., Gouard, S., Collet, M., 2011. Cytotoxic effect of hyperthermia and chemotherapy with platinum salt on ovarian cancer cells: results of an in vitro study. Eur. Surg. Res. 46, 139–147.
Mustafa, S., Elgazzar, A.H., Essam, H., Gopinath, S., Mathew, M., 2007. Hyperthermia alters kidney function and renal scintigraphy. Am. J. Nephrol. 27 (3), 315–321.
Ortega-Deballon, P., Facy, O., Jambet, S., Magnin, G., Cotte, E., Beltramo, J.L., et al., 2010. Which method to deliver hyperthermic intraperitoneal chemotherapy with oxaliplatin? An experimental comparison of open and closed techniques. Ann. Surg. Oncol. 17 (7), 1957–1963.
Pelz, J.O., Doerfer, J., Hohenberger, W., Meyer, T., 2005. A new survival model for hyperthermic intraperitoneal chemotherapy (HIPEC) in tumor-bearing rats in the treatment of peritoneal carcinomatosis. BMC Cancer 5, 56.
Pérez-Ruixo, C., Valenzuela, B., Peris, J.E., Bretcha-Boix, P., Escudero-Ortiz, V., Farré-Alegre, J., et al., 2013a. Population pharmacokinetics of hyperthermic intraperitoneal oxaliplatin in patients with peritoneal carcinomatosis after cytoreductive surgery. Cancer Chemother. Pharmacol. 71 (3), 693–704.
Pérez-Ruixo, C., Valenzuela, B., Peris, J.E., Bretcha-Boix, P., Escudero-Ortiz, V., Farré-Alegre, J., et al., 2013b. Neutrophil dynamics in peritoneal carcinomatosis patients treated with cytoreductive surgery and hyperthermic intraperitoneal oxaliplatin. Clin. Pharmacokinet. 52 (12), 1111–1125.
Pérez-Ruixo, C., Peris, J.E., Escudero-Ortiz, V., Bretcha-Boix, P., Farré-Alegre, J., Pérez-Ruixo, J.J., et al., 2014. Rate and extent of oxaliplatin absorption after hyperthermic intraperitoneal administration in peritoneal carcinomatosis patients. Cancer Chemother. Pharmacol. 73 (5), 1009–1020. http://dx.doi.org/10.1007/s00280-014-2436-6.
Pérez-Ruixo, C., Valenzuela, B., Peris, J.E., Bretcha-Boix, P., Escudero-Ortiz, V., Farré-Alegre, J., et al., 2016. Platelet dynamics in peritoneal carcinomatosis patients treated with cytoreductive surgery and hyperthermic intraperitoneal oxaliplatin. AAPS J. 18 (1), 239–250.
Pestieau, S.R., Stuart, O.A., Chang, D., Jacquet, P., Sugarbaker, P.H., 1998. Pharmacokinetics of intraperitoneal gemcitabine in a rat model. Tumori 84 (6), 706–711.
Pestieau, S.R., Belliveau, J.F., Griffin, H., Stuart, O.A., Sugarbaker, P.H., 2001. Pharmacokinetics of intraperitoneal oxaliplatin: experimental studies. J. Surg. Oncol. 76 (2), 106–114.
Piché, N., Leblond, F.A., Sidéris, L., Pichette, V., Drolet, P., Fortier, L.-P., et al., 2011. Rationale for heating oxaliplatin for the intraperitoneal treatment of peritoneal carcinomatosis: a study of the effect of heat on intraperitoneal oxaliplatin using a murine model. Ann. Surg. 254, 138–144.
R Core Team, 2016. R: A Language and Environment for Statistical Computing. R Foundation for Statistical Computing, Vienna, Austria. https://www.r-project.org/.
Rietbroek, R.C., van der Vaart, P.J., Haveman, J., Blommaert, F.A., Geerdink, A., Bakker, P.J., et al., 1997. Hyperthermia enhances the cytotoxicity and platinum-DNA adduct formation of lobaplatin and oxaliplatin in cultured SW 1573 cells. J. Cancer Res. Clin. Oncol. 123, 6–12.
Robella, M., Vaira, M., De Simone, M., 2016. Safety and feasibility of pressurized intraperitoneal aerosol chemotherapy (PIPAC) associated with systemic chemotherapy: an innovative approach to treat peritoneal carcinomatosis. World J. Surg. Oncol. 29 (14), 128.
Roberts, M.S., Magnusson, B.M., Burczynski, F.J., Weiss, M., 2002. Enterohepatic circulation: physiological, pharmacokinetic and clinical implications. Clin. Pharmacokinet. 41, 751–790.
RStudio Team, 2015. RStudio: Integrated Development for R. RStudio, Inc., Boston, MA (URL).
van Ruth, S., Mathôt, R.A.A., Sparidans, R.W., Beijnen, J.H., Verwaal, V.J., Zoetmulder, F.A.N., 2004. Population pharmacokinetics and pharmacodynamics of mitomycin during intraoperative hyperthermic intraperitoneal chemotherapy. Clin. Pharmacokinet. 43 (2), 131–143.
Savic, R.M., Karlsson, M.O., 2009. Importance of shrinkage in empirical bayes estimates for diagnostics: problems and solutions. AAPS J. 11 (3), 558–569.
Savic, R.M., Jonker, D.M., Kerbusch, T., Karlsson, M.O., 2007. Implementation of a transit compartment model for describing drug absorption in pharmacokinetic studies. J. Pharmacokinet. Pharmacodyn. 34 (5), 711–726.
Sladen, R.N., 1987. Effect of anesthesia and surgery on renal function. Crit. Care Clin. 3, 373–393.
Sørensen, O., Andersen, A.M., Kristian, A., Giercksky, K.-E., Flatmark, K., 2014. Impact of hyperthermia on pharmacokinetics of intraperitoneal mitomycin C in rats investigated by microdialysis. J. Surg. Oncol. 109 (6), 521–526.
Sticca, R.P., Dach, B.W., 2003. Rationale for hyperthermia with intraoperative intraperitoneal chemotherapy agents. Surg. Oncol. Clin. N. Am. 12 (3), 689–701.
Sugarbaker, P.H., 2005. Strategies for the prevention and treatment of peritoneal carcinomatosis from gastrointestinal cancer. Cancer Investig. 23, 155–172.
Sugarbaker, P.H., Van der Speeten, K., 2016. Surgical technology and pharmacology of hyperthermic perioperative chemotherapy. J. Gastrointest. Oncol. 7 (1), 29–44.
Sugarbaker, P.H., Averbach, A.M., Jacquet, P., Stephens, A.D., 1996. A simplified approach to hyperthermic intraoperative intraperitoneal chemotherapy (HIIC) using a self retaining retractor. Cancer Treat. Res. 82, 415–421.
Valenzuela, B., Nalda-Molina, R., Bretcha-Boix, P., Escudero-Ortíz, V., Duart, M.J., Carbonell, V., et al., 2011. Pharmacokinetic and pharmacodynamic analysis of hyperthermic intraperitoneal oxaliplatin-induced neutropenia in subjects with peritoneal carcinomatosis. AAPS J. 13 (1), 72–82.
Verwaal, V., van Ruth, S., de Bree, E., van Slooten, G.W., van Tinteren, H., Boot, H., et al., 2003. Randomized trial of cytoreduction and hyperthermic intraperitoneal chemotherapy versus systemic chemotherapy and palliative surgery in patients with peritoneal carcinomatosis of colorectal cancer. J. Clin. Oncol. 21, 3737–3743.
Wahlby, U., Jonsson, E.N., Karlsson, M.O., 2002. Comparison of stepwise covariate model building strategies in population pharmacokinetic-pharmacodynamic analysis. AAPS PharmSci 4, E27.
Yonemura, Y., Fujimura, T., Nishimura, G., null, FallaR, Sawa, T., Katayama, K., et al., 1996. Effects of intraoperative chemohyperthermia in patients with gastric cancer with peritoneal dissemination. Surgery 119 (4), 437–444.
Zakris, E.L., Dewhirst, M.W., Riviere, J.E., Hoopes, P.J., Page, R.L., Oleson, J.R., 1987. Pharmacokinetics and toxicity of intraperitoneal cisplatin combined with regional hyperthermia. J. Clin. Oncol. 5 (10), 1613–1620.